 CMC, vol.37, no.1, pp.39-57, 2013

Design of Aligned Carbon Nanotubes Structures Using Structural Mechanics Modeling Part 1: Theory and Individual Carbon Nanotube Modeling

J. Joseph[1] **and Y. C. Lu**[1]

Abstract: Aligned carbon nanotubes structures are emerging new materials that have demonstrated superior mechanical, thermal, and electrical properties and have the huge potential for a wide range of applications. In contrast with traditional materials whose microstructures are relatively "fixed", the aligned carbon nanotube materials have highly "tunable" structures. Therefore, it is crucial to have a rational strategy to design and evaluate the architectures and geometric factors to help process the optimal nanotube materials. Astructural mechanics based computational modeling is used for designing the aligned carbon nanotubes structures. Part 1 of the papers presents the theory of the computational method as well as the design and modeling of individual nanotube. As the fundamental building block of the aligned nanotube structures, the variations of geometric parameters of the individual nanotube on its mechanical properties are thoroughly examined.

Keywords: Aligned carbon nanotubes, Nanotubes, Finite element method.

1 Introduction

Since its discovery in the early 90's [Iijima (1991, 1993)], carbon nanotube (CNT) has continued to attract great interest due to its superior structures and properties. An individual single-walled CNT may be visualized as originating from a single layer sheet of graphene rolled up to form a tube structure. Depending on the directions of rolling vectors, the CNT can be in different configurations, i.e., armchair, zigzag, and chiral. Carbon nanotube can also be in multi-walled structure, with consists of a group of coaxial single-walled carbon nanotubes. Like diamond, carbon nanotube is also allotrope of carbon. A carbon atom in a CNT has six electrons with two of them filling the 1s orbital and the other four filling the sp^2 orbital. The rolled structure of CNT causes $\sigma - \pi$ rehybridization in which the three σ bonds are slightly out of plane, which makes the π orbital more delocalized outside the

[1] Department of Mechanical Engineering, University of Kentucky, Lexington, KY, U.S.A

nanotube. This has resulted in extremely strong carbon nanotubes, with possibly the highest Young's modulus and tensile strength. There have been numerous theoretical studies on the mechanical properties of an individual carbon nanotube [Krishnan et al. (1998); Wong et al. (1997); Lu (1997); Popov et al. (2000); Zhan and Gu (2011); Zeng (2011)], and the Young's modulus and shear modulus of a CNT have been predicted to be as high as 1.25 TPa and 0.45 TPa, respectively. Due to the small dimensions, the actual measurements on the properties of an individual CNT has proven to be difficult. Treacy et al. have carried out the first successful measurement of the Young's modulus of individual CNT. By thermally inducing a vibration on a CNT cantilever inside a transmission electron microscope, they have reported the Young's modulus of a multi-walled CNT as 1.8 TPa [Treacy et al. (1996)]. Wong et al. (1997) have reported for multiwalled CNTs Young's Modulus values of 0.69 - 1.87 TPa by using an AFM to bend the CNT. Yu et al. (2000) have conducted nanoscale tensile test of a CNT by pulling the tip with an AFM and observing it under SEM and reported Young's modulus in the range 0.27 - 0.95 TPa.

Due to its small sizes (the tube diameter is only a few nanometers), a single carbon nanotube has very limited applications. Most devices would require that the carbon nanotube be produced in large scales and at oriented forms. These have resulted in a new form of carbon nanotubes: the aligned carbon nanotubes (A-CNTs) structures. As sketched in Fig.1a, an A-CNT structure is comprised of numerous individual CNTs adhered vertically to a flat substrate. The A-CNT structure was first fabricated by Terrones et al. [Terrones et al. (1997)] through the method of laser ablation. Latest technologies such as the chemical vapor deposition (CVD) method have made it possible to produce the aligned CNTs at much large scales. The aligned carbon nanotubes structures have found a wide range of applications in areas such as electrical interconnects [Kreupl et al. (2002)], thermal interfaces [Cola (2009)], energy dissipation devices [Liu et al. (2008)], microelectronic devices [Fan et al. (1999)], and flow sensors on micro air vehicles [Zhang et al. (2010)], etc.

Unlike traditional materials (metals, ceramics and polymers) whose microstructures are relatively "fixed", the aligned carbon nanotube materials have highly "tunable" structures. The optimal performance (thermal, electrical and mechanical) of the A-CNTs highly depend upon their architectures and geometric parameters, including the tube height, tube diameter, tube array density, tube distribution pattern, inter-tube distance, tube-tube junction structure, and among many other factors. Therefore, it is crucial to have a rational strategy to design and evaluate the architectures and geometric factors to help process the optimal nanotube materials.A review of literature on carbon nanotubes has revealed that extensive works avail-

able so far are on modeling and characterization of individual CNT as against fewer works available/published on modeling and characterization of the A-CNT structures. The most commonly used method for modeling the individual CNT has been the atomistic approach, which includes the classical molecular dynamics [Cornwell and Wille (1997); Popov et al. (2000)], tight binding molecular dynamics [Hernandez et al. (1998, 1999)], and density functional theory [Sanchez-Portal et al. (1999)]. Although the atomistic approach is successful for handling an individual nanotube, it is too computational expensive for modeling an aligned CNT structure that is consisted of millions or even billions of individual tubes in a square centimeters. The present papers present a frame work for designing and modeling the aligned carbon nanotubes structures by using the structural mechanics approach, i.e., the finite element method. Part 1 presents the theory and the modeling of an individual nanotube, which is the fundamental building block of the aligned nanotube structures. Part 2 presents the detailed design and modeling of the aligned carbon nanotube structures.

2 Modeling Procedures for Individual Carbon Nanotubes

2.1 Finite Element Formulation

The approach in this work is based on the principle of structural mechanics (finite element method (FEM)). As illustrated in Fig.1a, an aligned carbon nanotubes structure is composed of numerous individual nanotubes that are packed vertically on flat substrates. Each individual carbon nanotube may be understood as geometrical space frame structures with primary bonds between any two neighboring atoms acting as load bearing members and the atoms may be visualized as joints for these load bearing members (Fig.1b). Therefore, the 3D space beam elements were deemed to be appropriate and effective for modeling the carbon nanotubes structures (Fig.1c). The general purpose finite element programs are often based on displacement or stiffness based finite element formulation, wherein the governing equations are expressed in terms of nodal displacements using equations of equilibrium describing the behavior of an element in matrix form and represented as below [Logan (2002)].

$$\{f\}^e = [k]^e \{q\}^e \tag{1}$$

where

$[k]^e =$ Element stiffness matrix

$\{q\}^e =$ Element displacement vector

$\{f\}^e =$ Element force vector

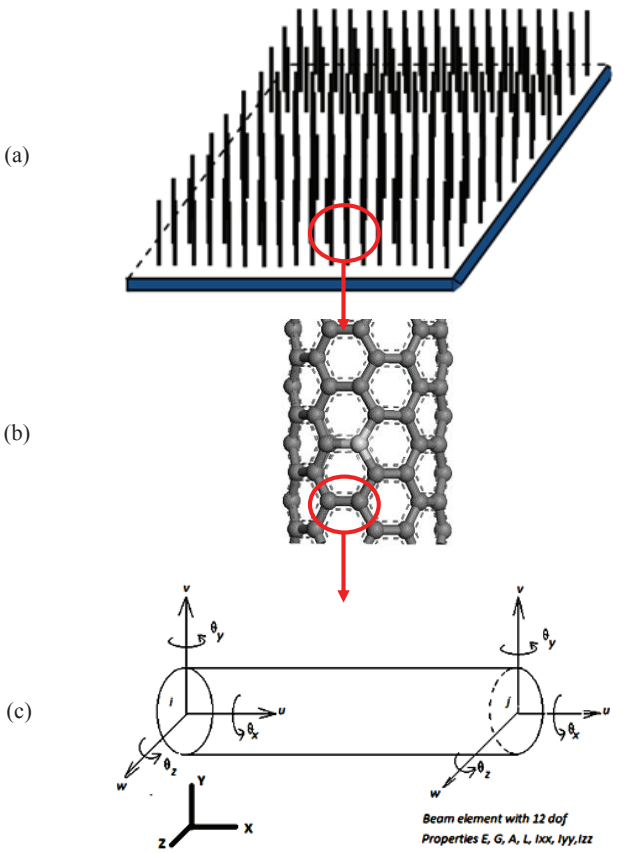

Figure 1: (a) A sketch for align carbon nanotubes structure (not to scale); (b) A sketch for an individule carbon nanotube; and (c) A 3D beam element in space.

For a beam element that is arbitrarily oriented in space as shown in Fig.1c, the stiffness matrices considering bending about two axes $\hat{y}$ (for bending in $\hat{x}-\hat{z}$ plane) and $\hat{z}$ (for bending in $\hat{x}-\hat{y}$ plane), upon direct superposition with the axial stiffness matrix & the torsional stiffness matrix yields the element stiffness matrix $[k]^e$ for the beam element in 3-D space as below.

$$[k]^e = \begin{bmatrix} k_{ii} & k_{ij} \\ k_{ji} & k_{jj} \end{bmatrix} \tag{2}$$

where

$$k_{ii}=\begin{bmatrix} \frac{EA}{L} & & & & & \\ 0 & \frac{12EI_{zz}}{L^3} & & & \textit{Symmetric} & \\ 0 & 0 & \frac{12EI_{yy}}{L^3} & & & \\ 0 & 0 & 0 & \frac{GJ}{L} & & \\ 0 & 0 & \frac{-6EI_{yy}}{L^2} & 0 & \frac{4EI_{yy}}{L} & \\ 0 & \frac{6EI_{zz}}{L^2} & 0 & 0 & 0 & \frac{4EI_{zz}}{L} \end{bmatrix}$$

$$k_{jj}=\begin{bmatrix} \frac{EA}{L} & & & & & \\ 0 & \frac{12EI_{zz}}{L^3} & & & \textit{Symmetric} & \\ 0 & 0 & \frac{12EI_{yy}}{L^3} & & & \\ 0 & 0 & 0 & \frac{GJ}{L} & & \\ 0 & 0 & \frac{6EI_{yy}}{L^2} & 0 & \frac{4EI_{yy}}{L} & \\ 0 & \frac{-6EI_{zz}}{L^2} & 0 & 0 & 0 & \frac{4EI_{zz}}{L} \end{bmatrix}$$

$$k_{ij}=\begin{bmatrix} \frac{-EA}{L} & 0 & 0 & 0 & 0 & 0 \\ 0 & \frac{-12EI_{zz}}{L^3} & 0 & 0 & 0 & \frac{6EI_{zz}}{L^2} \\ 0 & 0 & \frac{-12EI_{yy}}{L^3} & 0 & \frac{-6EI_{yy}}{L^2} & 0 \\ 0 & 0 & 0 & \frac{-GJ}{L} & 0 & 0 \\ 0 & 0 & \frac{6EI_{yy}}{L^2} & 0 & \frac{2EI_{yy}}{L} & 0 \\ 0 & \frac{-6EI_{zz}}{L^2} & 0 & 0 & 0 & \frac{2EI_{zz}}{L} \end{bmatrix}$$

and $k_{ji} = k_{ij}^T$

The corresponding element displacement and force vectors are

$$\{q\}^e = [u_i, v_i, w_i, \theta_{xi}, \theta_{yi}, \theta_{zi}, u_j, v_j, w_j, \theta_{xj}, \theta_{yj}, \theta_{zj}]^T$$

$$\{f\}^e = [f_{xi}, f_{yi}, f_{zi}, m_{xi}, m_{yi}, m_{zi}, f_{xj}, f_{yj}, f_{zj}, m_{xj}, m_{yj}, m_{zj}]^T$$

The element stiffness equation is established for each of the beam element in the space frame followed by appropriate transformation of reference frame from local to global coordinate system and solution to nodal displacement. The individual element equations are then added together using a method of superposition referred to as direct stiffness method in order to obtain the global equations for the whole aligned nanotubes structure with the final assembled/global equation

$$\{F\} = [K]\{Q\} \tag{3}$$

where

$[K]$ = Structure global stiffness matrix

$\{Q\}$ = Vector of generalized displacements

$\{F\}$ = Vector of global nodal forces

The system of simultaneous linear equations can then be solved by applying boundary conditions to obtain the nodal force, displacements, and element stresses.

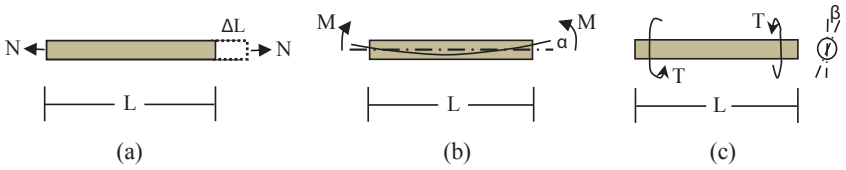

Figure 2: Sketches showing a beam under (a) pure tension, (b) bending and (c) torsion.

It is generally accepted that the C-C bonds in a carbon nanotube are circular in cross section. From structural mechanics principles, the expression for strain energy of a uniform beam subjected to a pure axial force 'N' as shown in Fig.2(a) is given by

$$U_N = \frac{1}{2}\iiint \sigma_x \varepsilon_y dV = \frac{1}{2}\left(\frac{EA}{L}\right)(\Delta L)^2 \tag{4}$$

where 'ΔL' is the axial deformation due to stretching.

Similarly the strain energy of a beam subject to pure bending moment 'M' as shown in Fig.2(b) is given by

$$U_M = \frac{1}{2}\iiint \sigma_b \varepsilon_b dV = \frac{1}{2}\left(\frac{EI}{L}\right)(2\alpha)^2 \tag{5}$$

where 'α' is the rotation due to bending.

Further, the strain energy of a beam subject to pure torsional moment 'T' as shown in Fig.2(c), developing circumferential shear stress 'τ' and corresponding shear strain 'γ' is given by

$$U_T = \frac{1}{2}\iiint \tau\gamma dV = \frac{1}{2}\left(\frac{GJ}{L}\right)(\Delta\beta)^2 \tag{6}$$

where '$\Delta\beta$' is the torsional rotation.

By comparing the above strain energy equations with the steric potential energy equations obtained from molecular mechanics [Cornell et al. (1995)], the structural beam parameters can be related to the molecular force constants as follows

$$k_a = \frac{EA}{L}; \quad k_\theta = \frac{EI}{L}; \quad k_\tau = \frac{GJ}{L} \tag{7}$$

Assuming a circular cross-section for the C-C- bond beam with a diameter d, the geometric properties become A=$\pi d^2/4$, I=$\pi d^4/64$, and J=$\pi d^4/32$. Substituting them into Eq.7 yield

$$d = 4\sqrt{\frac{k_\theta}{k_r}}; \quad E = \frac{k_r^2 L}{4\pi k_\theta}; \quad G = \frac{k_r^2 k_\tau L}{8\pi k_\theta^2} \tag{8}$$

The force constants values were selected as k_a = 938 Kcal mol^{-1} Å^{-2}, k_θ = 126 Kcal mol^{-1}rad^{-2} and k_τ = 40 Kcal mol^{-1}rad^{-2} [Cornell et al. (1995)]. Using these values, the elastic modulus of the C-C bond beams can be calculated and then used in the finite element analysis for the nanotube structures.

2.2 FE Models of Individual Carbon Nanotubes

The CNTs are classified into three types: (i) armchair, (ii) zigzag, and (iii) chiral. It is noticed that when the chiral angles become 0° and 30°, the chiral CNT essentially becomes the zigzag and armchair tubes, respectively. Therefore, the CNTs with zigzag and armchair configurations were the primary concern in the present study. First, individual carbon nanotube in zigzag and armchair configurations were geometrically modeled using the modeling capability of ANSYS software. The solid nanotube models were then imported into ABAQUS CAE where the nanotube models were meshed using 3D beam elements (Fig.3). Both linear (B31) and quadratic (B32) formulation beam elements were used in the analyses. Appropriate beam section orientation, geometric sectional properties, and material properties obtained from the molecular-structural correlation were implemented. The thickness of the nanotube was varied from 0.066 nm to 0.69 nm. The beam elements were modeled assuming circular cross sections for which the diameters were assigned equivalent to the values of the thickness identified. The diameter of the overall nanotube was varied between 0.5 nm - 2.5 nm. The nanotubes were subjected to tensile loading by way of imposing displacements at the free ends and with the other ends of the nanotubes constrained in all the degrees of freedom. Analyses were run by varying the mesh size, i.e., by varying the number of elements in the nanotube FE models. Hence a convergence study was conducted before arriving at the final results.

3 Results and Discussion

3.1 Variation of Young's Modulus with Nanotube Wall Thickness

The individual nanotube is the fundamental building block of the aligned nanotube structures, therefore, the structure and properties of the individual are first analyzed. The complete FE model for the individual nanotubes were setup in the FE software

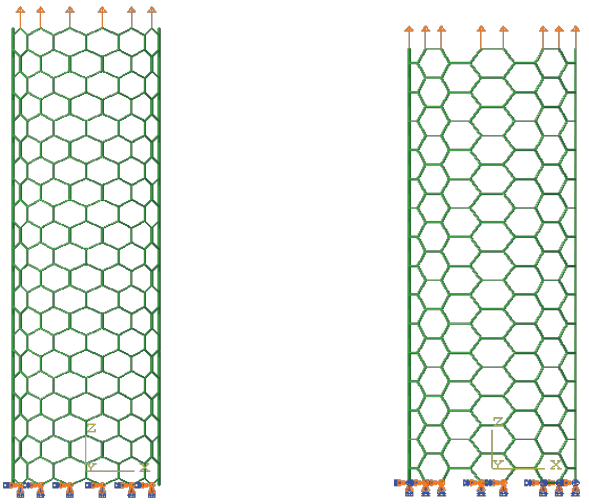

Figure 3: Finite element models for individual carbon nanotube (CNT) at (a) zigzag (14, 0) configuration and (b) armchair (8,8) configuration.

ABAQUS with appropriately calculated beam properties for the C-C bonds of the nanotubes. The effect of nanotube wall thickness on the Young's modulus of the carbon nanotube was evaluated. Several values of nanotube thickness have been reported in the literature. In this analysis, the commonly reported values of thickness viz. 0.066 nm [Krishnan et al. (1998)], 0.075 nm [Wong et al. (1997)], 0.147 nm [Salvetat et al. (1999)], 0.154 nm (which is the diameter of carbon atom), and 0.34 nm (which is the interwall spacing of graphite) have been used for modeling the nanotubes. The Young's modulus of the nanotube structure is then evaluated using the relation

$$E = \frac{PL}{A\delta} \tag{9}$$

where

$P =$ Applied load

$\delta =$ Elongation of the nanotube

$L =$ Length of the nanotube

$A =$ Cross sectional area of the nanotube

A convergence study was first conducted by using linear beam elements (B31) having linear displacement function as well as using quadratic beam elements (B32) having 3 nodes /quadratic displacement function and by varying the mesh size. Fig.4 shows the plot of convergence of Young's modulus for a zigzag (14, 0) nanotube with the increase in number of nodes. It is seen that a coarse FE mode (fewer nodes) would yield inaccurate results. Fig.5 shows the results of combining both the variation of 'E' with nanotube thickness as well as with higher order elements and with increased number of elements. It is seen that the Young's modulus of the nanotubes decreases in a linear fashion with increasing nanotube wall thickness. This trend has been observed in several works reported in the literature while the exact values are widely scattered [Lu (1997); Prylutskyy et al. (2000); Popov et al. (2000)]. The graph also shows the mesh convergence behavior of the nanotube FE model. It is evident that the results of analysis obtained when modeled with element type "linear beam" using four elements approaches the results obtained when modeled with "quadratic beam" using two elements. Thus it can be concluded that the Young's modulus of the nanotube is sensitive to the wall thickness, consistent with the works reported in the literature.

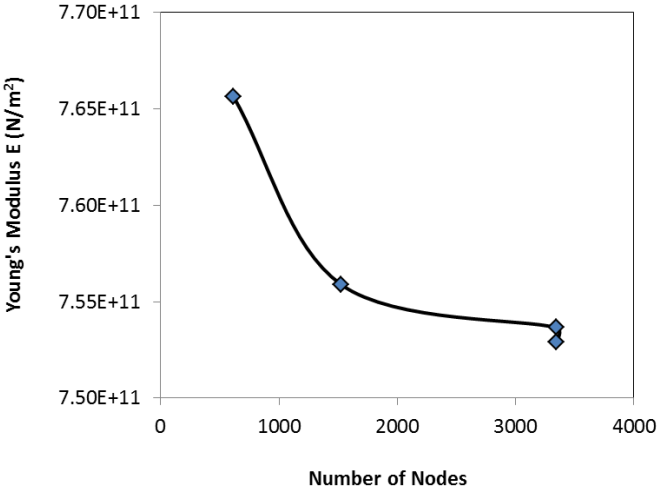

Figure 4: Convergence of Young's modulus nanotube of the nanotube with the number of nodes. The nanotube used is the zigzag (14, 0) structure.

Furthermore, it is observed that the Young's modulus of the nanotube at armchair configuration is slightly higher than that at zigzag configuration (Fig.6). The difference becomes magnified when the wall thickness of the nanotube is small. This is mostly attributed by the positions of the hexagonal carbon rings in the two types

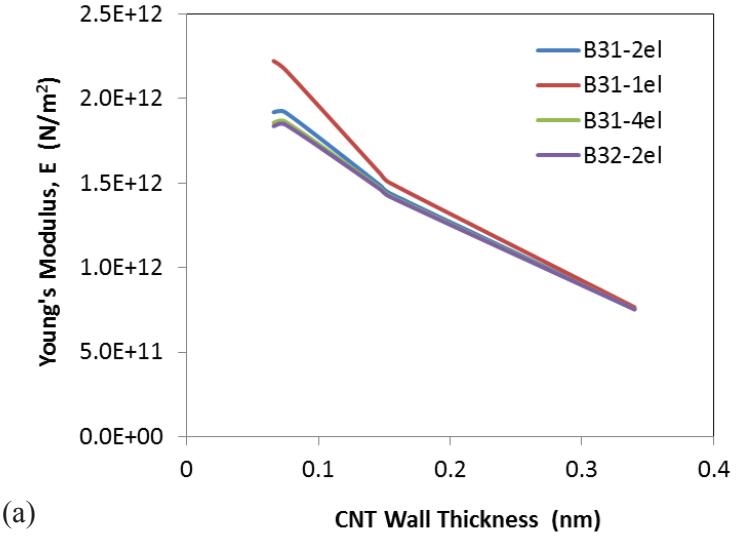

(a)

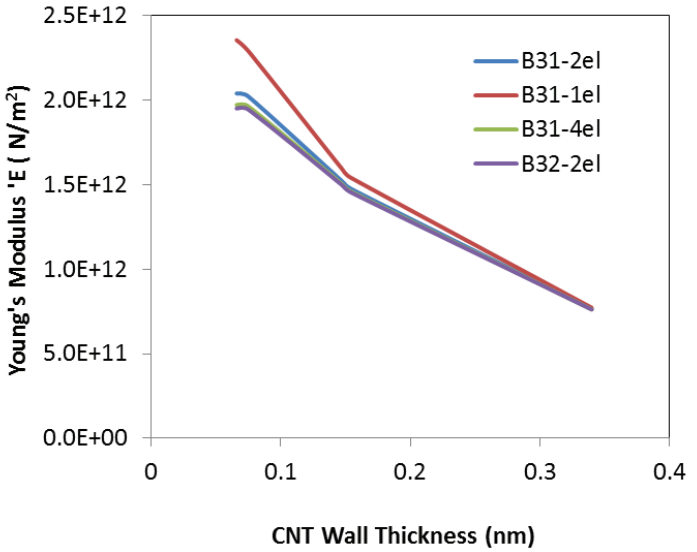

(b)

Figure 5: Variation of Young's modulus as a function of nanotube wall thickness for (a) zigzag (14, 0) CNT and (b) armchair (8, 8) CNT.

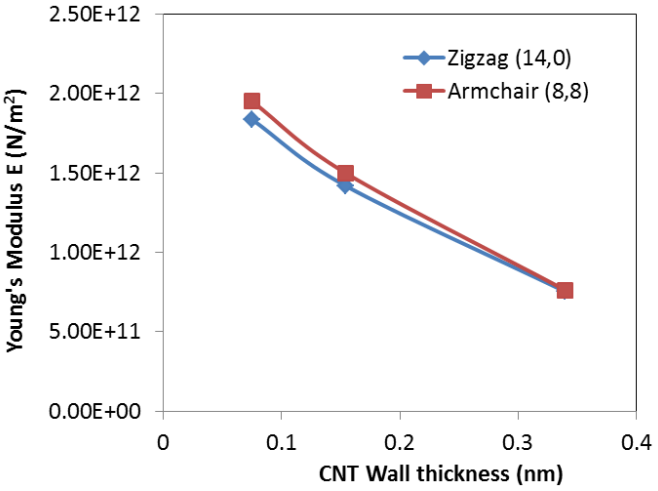

Figure 6: Comparison of Young's modulus from two different CNT configurations. Results are obtained by using 3-node, quadratic beam elements (B32).

of nanotubes, as illustrated in Fig.3. Consider a single hexagonal carbon ring in both tubes: when subjected to axial loading (tension or compression), the load in armchair tube is carried by the two horizontal arms while the load in zigzag tube is only carried by two vertices. Therefore, the nanotube in armchair structure may be stronger than the naotube in zigzag structure.

3.2 Variation of Young's Modulus with Poisson's Ratio

By structural mechanics analogy, we visualize the bond between any two neighboring carbon atoms as a space frame structure. The effect of Poisson's ratio of this C-C bond on the Young's modulus of the nanotube is studied. Similar to the several values of thickness reported in the literature, an equally good number of values of Poisson's ratio have been reported as well [Lu (1997); Chang and Gao (2003); Zhao and Shi (2011)]. Values of Poisson's ratio viz. 0.16, 0.19, 0.22, 0.30 and 0.49 have been commonly observed. With these Poisson's ratio values, the Young's modulus of the nanotubes are evaluated. The results are displayed in Fig.7 for both zigzag and armchair configurations. Overall, the Young's modulus of the nanotubes is seen to decrease linearly with increasing values of Poisson's ratio. Once again, it is observed that the Young's modulus of the nanotube at armchair configuration is higher than that at zigzag configuration, consistent with the trend obtained earlier by varying the nanotube wall thickness (Fig.6).

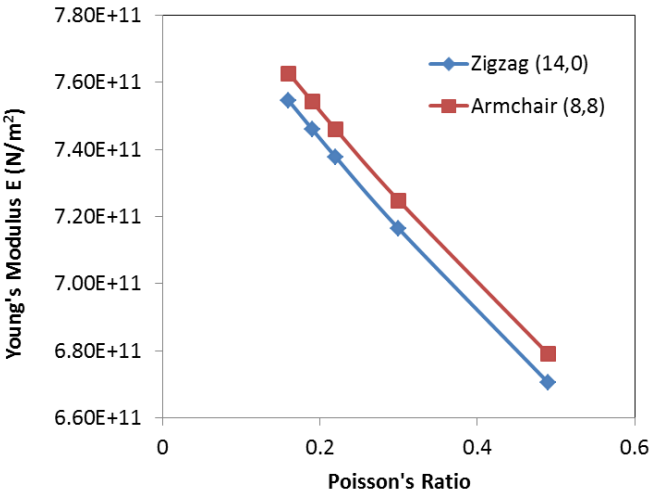

Figure 7: Variation of Young's modulus as a function of nanotube Poisson's ratio for both zigzag and armchair configurations.

3.3 Variation of Nanotube Young's Modulus with Nanotube Diameter

One of the key parameters in designing a carbon nanotube is its diameter. In present study, nanotubes in the diameter range from 0.392 nm to 2.351 nm were considered in order to evaluate the variation of elastic modulus with the nanotube diameter. The wall thickness of these nanotubes was fixed at 0.34 nm, which is one of the widely accepted values in the literature. It may be noted that the value of this thickness assigned to small diameter nanotubes is contradictory since the thickness is close to the diameter as already has been pointed out by several researchers in the nanotube community. However this scenario was still included for the analyses in this work to observe a general trend. The carbon nanotube FE models with diameter variation from 0.392 nm until 2.351 nm were set up for tensile loading experiment in ABAQUS. The material properties for the beam material simulating the bonds were based on the initially evaluated values that were obtained upon equivalence of molecular and structural mechanics parameters. The Poisson's ratio value of 0.16 was applied for the carbon bonds as discussed in previous analysis. Beam element (B32) with quadratic interpolation having three displacement and three rotation degrees of freedom at each node was used. The nanotube was first subjected to an axial displacement and a linear static analysis with NLGEOM= OFF was conducted and the resulting reaction forces were evaluated. From these uniaxial loading experiments, the Young's modulus (E) of the nanotubes at various nanotube diameters were evaluated by using Eq. 9.

Fig.8(a) shows the displacement contour along the length of a zigzag (14, 0) nanotube upon subjecting it to an axial displacement. The evaluated values of Young's modulus of several zigzag nanotubes are plotted as seen in Fig.8(b). As may be observed from the graph the Young's modulus starts with a value of 0.74 TPa for the (5, 0) zigzag configuration and increases almost linearly until a value of 0.753 TPa for the (8, 0) zigzag configuration beyond which the value of Young's modulus almost stabilizes there until for the (11, 0) zigzag configuration and further increases to 0.757 TPa for nanotube diameters of 1.646 nm and beyond. The Young's modulus of the zigzag configuration nanotubes increases at a much steeper rate with diameter for small diameter nanotubes as compared to large diameter nanotubes. The trend and values obtained are in close agreement with several results reported in the literature [Lu (1997); Prylutskyy et al. (2000); Popov et al. (2000)].

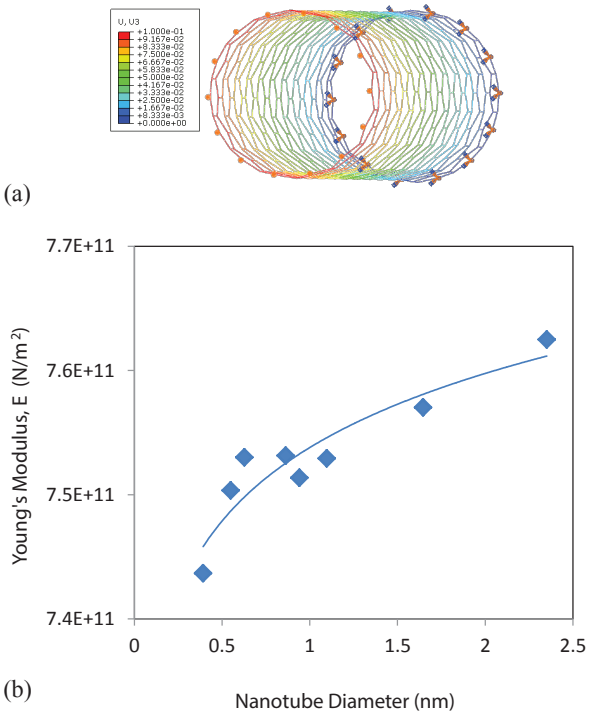

Figure 8: (a) Deformation contour of a zigzag CNT under tension; (b) Variation of Young's modulus as a function of nanotube diameter for a zigzag CNT.

3.4 Variation of Nanotube Shear Modulus with Nanotube Diameter

Continuing with a similar analysis as above, the shear modulus (G) of the carbon nanotubes at various nanotube diameters were evaluated. The thickness of nanotube used was set as 0.34 nm, same as used in previous analysis. The zigzag CNT FE models with diameter variation from 0.392 nm to 2.351 nm are set up for torsion experiment in ABAQUS. The nanotubes were subjected to a torsional moment and linear static analysis with NLGEOM= OFF were conducted. From the analysis, the resulting twist angles of the nanotubes were evaluated. The shear modulus (G) of the nanotubes were computed by using Eq. 10.

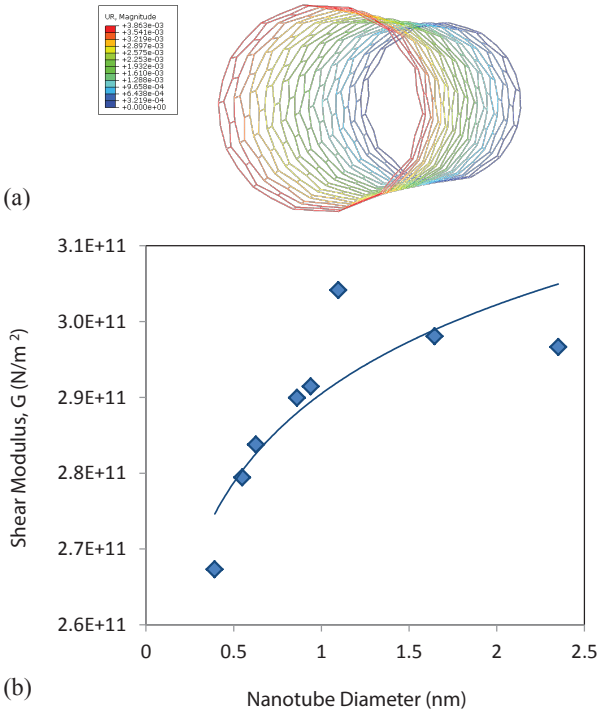

Figure 9: (a) Deformation contour of a zigzag CNT under torsion; (b) Variation of shear modulus as a function of nanotube diameter for a zigzag CNT.

$$G = \frac{TL}{J\theta} \tag{10}$$

where

T = Torque applied to the nanotube

L = Length of the nanotube

J = Polar moment of inertia of nanotube

θ = Angle of twist of the nanotube

Fig.9(a) shows the displacement contour of a nanotube subject to a torsional load. The evaluated values of shear modulus of several zigzag nanotubes are plotted as seen in Fig.9(b). As may be observed from the graph, the shear modulus starts with 0.267 TPa for the (5, 0) zigzag configuration and increases almost linearly until 0.304 TPa for the (14, 0) zigzag configuration beyond which the value of shear modulus almost stabilizes at around 0.30 TPa for nanotube diameters up to 2.5 nm and beyond, approaching close to that of shear modulus of graphite. In general, the shear modulus of the nanotubes increases with diameter for small diameter nanotubes and tends to become constant for large diameter nanotubes.

3.5 Variation of Young's Modulus with Nanotube Length

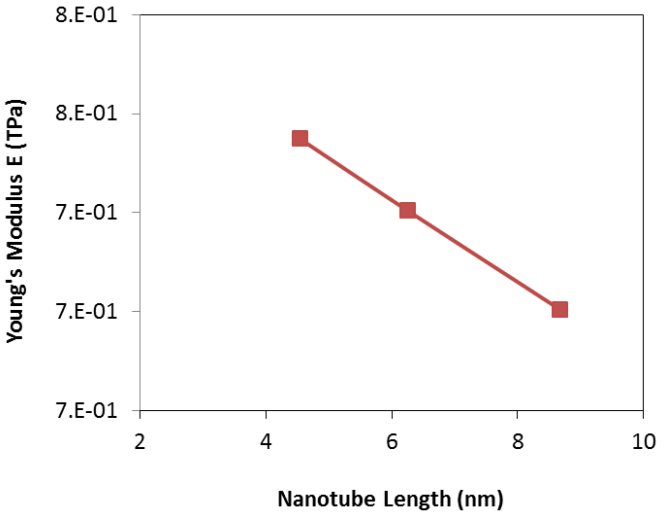

Figure 10: Variation of Young's modulus as a function of nanotube height.

Another key parameter in designing a carbon nanotube is its length or height. Experimentally, the length of the carbon nanotubes can be adjusted by controlling the

growth conditions such as temperature, time, and pressure. It is interested to know the effect of nanotube length on the resultant properties of the nanotube structures. In this study, the FE models for nanotubes with various lengths (heights) were constructed and the elastic modulus were evaluated. The nanotubes used were in zigzag configuration with a fixed wall thickness of 0.34 nm. The effect of nanotube length on Young's modulus is depicted in Fig.10. Overall trend indicates an almost linear relationship between the modulus and the length. The higher the nanotube, the lower the modulus. The overall trend is consistent with the classical Euler's beam buckling equation, where the buckling force is inversely proportional to the beam length.

4 Summary

The structural mechanics based computational modeling has been used to design and characterize the individual carbon nanotubes, which are the fundamental building block of aligned carbon nanotubes structure. Based on an understanding of carbon nanotubes at the atomic/molecular level, the equivalent truss structure models of the CNTs were constructed by using space beam elements. The geometric parameters of the individual nanotube on its mechanical properties are thoroughly examined. It is observed that the Young's modulus and shear modulus of the nanotube are sensitive to the atomic structure of the tubes, where the CNTs in armchair configuration generally have higher stiffness than the CNTs in zigzag one. The strength of the CNTs further depends upon the diameter of the C-C bonds (tube wall thickness). As the wall thickness increases, the Young's modulus of the nanotubes decreases. The modulus of the nanotubes is also affected by the overall tube diameter. The Young's modulus generally increases at a much steeper rate with diameter for small diameter nanotubes and then becomes stabilized for large diameter nanotubes. Finally, the modulus of the nanotubes is inversely proportional to the tube length.

Acknowledgement

This work has been supported by the Kentucky NASA EPSCoR RIA program and the Kentucky Science and Engineering Foundation (KSEF) RDE program.

References

Chang, T.; Gao, H. (2003): Size-dependent elastic properties of a single-walled carbon nanotube via a molecular mechanics model. *Journal of the Mechanics and Physics of Solids,* vol. 51, no. 6, pp. 1059-1074.

Chen, H.; Roy, A.; Baek, J.-B.; Zhu, L.; Qu, J. ; Dai. L. (2010): Controlled growth and modification of vertically-aligned carbon nanotubes for multifunctional applications. *Materials Science and Engineering R-Reports,* vol. 70, pp. 63-91.

Ci, L.; Suhr, J.; Pushparaj, V.; Zhang, X.; Ajayan, P.M. (2008): Continuous carbon nanotube reinforced composites. *Nano Letters,* vol. 8, no. 9, pp. 2762-6.

Cola, B.A. (2009): Contact mechanics and thermal conductance of carbon nanotube array interfaces. *International Journal of Heat and Mass Transfer,* vol. 52, no. 15-16, pp. 3490–503.

Cornell, W.D.; Cieplak, P.; Bayly, C.I.; et al. (1995): A second generation force-field for the simulation of proteins, nucleic-acids, and organic-molecules. *Journal of American Chemical Society*, vol. 117, pp. 5179–5197.

Fan, S.; Chapline, M. G.; Franklin, N. R.; Tombler, T. W.; Cassell, A. M.; Dai, H. (1999): Self-oriented regular arrays of carbon nanotubes and their field emission properties. *Science*, vol. 283, pp. 512.

Hernandez, E.; Goze, C.; Bernier, P.; Rubio, A. (1998): Elastic properties of C and BxCyNz composite nanotubes. *Physical Review Letters*, vol. 80, pp. 4502–4505.

Hernandez, E.; Goze, C.; Bernier, P.; Rubio, A. (1999): Elastic properties of single-wall nanotubes. *Applied Physics A. Materials Science and Processing,* vol. 68, pp. 287–292.

Iijima, S. (1991): Helical microtubules of graphitic carbon. *Nature*, vol. 354, pp. 56–58.

Iijima, S.; Brabec, C.; Maiti, A.; Bernholc, J. (1996): Structural flexibility of carbon nanotubes. *Journal of Chemical Physics*, vol. 104, pp. 2089–2092.

Kreupl, G.A.P.; Duesberg, G. S.; Steinhogl, W.; Liebau, M.; Unger, E.; Honlein, W.; (2002): Carbon nanotubes in interconnect applications. *Microelectronic Engineering,* vol. 64, pp. 399–408.

Krishnan, A.; Dujardin, E.; Ebbesen, T.W.; Yianilos, P.N.; Treacy, M.M.J. (1998): Young's modulus of single-walled nanotubes. *Physical Review B*, vol. 58, pp. 14013–14019.

Liu, Y.; Qian, W. Z.; Zhang, Q.; Cao, A. Y.; Li, Z. F.; Zhou, W. P.; Ma, Y.; Wei, F. (2008): Hierarchical agglomerates of carbon nanotubes as high-pressure cushions. *Nano Letters,* vol. 8, pp. 1323.

Logan, D.L. (2002): *A First course in the Finite Element Method,* 3rd Ed, Thomson Asia Pte Ltd.

Lu, J.P. (1997): Elastic properties of carbon nanotubes and nanoropes. *Physical Review Letters,* vol. 79, pp. 1297–1300.

Popov, V.N.; Van Doren, V.E.; Balkanski, M. (2000): Elastic properties of single-walled carbon nanotubes. *Physical Review B*, vol. 61, pp. 3078–3084.

Prylutskyy, Y.I.; Durov, S.S.; Ogloblya, O.V.; Buzaneva, E.V.; Scharff, P. (2000): Molecular dynamics simulation of mechanical,vibrational and electronic properties of carbon nanotubes. *Computational Materials Science,* 17: p. 352–355.

Qu, L.; Zhao, Y.; Hu, Y.; Zhang, H.; Li, Y.; Guo, W.; Luo, H.; Dai. L. (2010): Controlled removal of individual carbon nanotubes from vertically-aligned carbon nanotube arrays for advanced nanoelectrodes. *Journal of Materials Chemistry,* vol. 20, pp. 3595.

Salvetat, J.P.; Briggs, G.A.D.; Bonard, J.M.; Bacsa, R.R.; Kulik, A.J.; Stockli, T.; Burnham, N.A.; Forro,L. (1999): Elastic and shear moduli of single-walled carbon nanotube ropes. *Physical Review Letters*, vol. 82, pp. 944–947.

Sanchez-Portal, D.; Artacho, E.; Soler, J.M. (1999): Ab initio structural, elastic, and vibrational properties of carbon nanotubes. *Physical Review B*, vol. 59, pp. 12678–12688.

Treacy, M.M.J.; Ebbesen, T.W.; Gibson, J.M.; (1996): Exceptionally high Young's modulus observed for individual carbon nanotubes. *Nature*, vol. 381, pp. 678–680.

Tu, Z.; Ou-Yang, Z. (2002): Single-walled and multiwalled carbon nanotubes viewed as elastic tubes with the elective Young's moduli dependent on layer number. *Physical Review B*, vol. 65, pp. 233407.

Tserpes, K.; Papanikos, P. (2005): Finite element modeling of single-walled carbon nanotubes. *Composites Part B: Engineering,* vol. 36, pp. 468-477.

Wong, E.W.; Sheehan, P.E.; Lieber, C.M. (1997): Nanobeam mechanics:elasticity, strength, and toughness of nanorods and nanotubes. *Science,* vol. 277, pp. 1971–1975.

Yakobson, B.; Brabec, C.; Bernholc, J. (1996): Nanomechanics of carbon tubes: instabilities beyond the linear response. *Physical Review Letters,* vol. 76, no. 14, pp. 2511–2514.

Yu, M.F.; Files, B.S.; Arepalli, S.; Ruoff, R.S. (2000): Tensile loading of ropes of single wall carbon nanotubes and their mechanical properties. *Physical Review Letters,* vol. 84, pp. 5552–5555.

Zhan, H.; Gu, Y. (2011): Atomistic exploration of deformation properties of copper nanowires with pre-existing defects. *Computer Modeling in Engineering & Sciences*, vol. 80, no. 1, pp. 23-56.

Zhang, Q.; Lu, Y.C.; Du, F.; Dai, L.; Baur, J.; Foster, D.C. (2010): Viscoelastic creep of vertically aligned carbon nanotubes. *Journal of Physics, D: Applied*

Physics, vol. 43, pp. 315401.

Zhao, P.; Shi, G. (2011): Study of Poisson Ratios of Single-Walled Carbon Nanotubes based on an Improved Molecular Structural Mechanics Model. *Computers Materials and Continua*, vol. 22, no. 2, pp. 147.

Zeng, X. (2011): Application of An Atomistic Field Theory to Nano/Micro Materials Modeling and Simulation. *Computer Modeling in Engineering and Sciences*, vol. 74, no. 3, pp. 183.